

Simulation-Driven Optimization of Metal Hydride-Packed Hydrogen Storage Systems for Enhanced Performance

Marco Maggini ¹, Andrea L. Facci ^{1*}, Giacomo Falcucci ², Stefano Ubertini ¹

¹ Department of Economics, Engineering, Society and Business Organization, University of Tuscia, 01100 Viterbo, Italy

² Department of Enterprise Engineering "Mario Lucertini", University of Rome "Tor Vergata", Via del Politecnico 1, 00133 Rome, Italy; John A. Paulson School of Engineering and Applied Physics, Harvard University, 33 Oxford Street, 02138 Cambridge, Massachusetts, USA.

(*Corresponding Author: andrea.facci@unitus.it)

ABSTRACT

Hydrogen, especially when stored within Metal Hydride (MH) containers, exhibits significant potential for energy storage. One of the primary challenges associated with using metal hydrides is their efficient thermal management. This can be addressed by incorporating an appropriate Phase Change Material (PCM) into the MH container, eliminating the need for additional active systems.

In this study, we perform numerical assessments on the performance of hybrid MH-PCM storage systems with varying aspect ratios. Numerical simulations indeed play a crucial role in designing, managing, and improving this technology. This evaluation aids in identifying instances where multi-dimensional phenomena can be disregarded, allowing simplified 1D models to be used.

We evaluate different cylindrical layouts of the hybrid MH-PCM hydrogen storage system concerning process duration, temperature distributions, and power. We identify a critical aspect ratio for the canister, beyond which relatively straightforward one-dimensional simulations can be employed without compromising outcomes. Moreover, we highlight that the overall time required for absorption and desorption reactions is not dramatically influenced by the discretization method, suggesting the practicality of relying on one-dimensional models especially when process evolution is not the focal point.

Keywords: renewable energy resources, hydrogen technologies, energy systems, hydrogen storage, phase change material, metal hydride

NONMENCLATURE

Abbreviations

RES	Renewable Energy Source
MH	Metal Hydride
PCM	Phase Change Material

Symbols

\mathcal{L}	Canister length
D	Inner cylinder (MH) diameter
b	Canister radius
ξ	Porosity
p	Pressure
eq	equilibrium
ρ	Density
c_p	Specific heat
m_{H_2}	Gaseous hydrogen
m_{MH}	Total hydride mass
r	Reaction rate
f	Mass flow rate
T	Temperature
k	Thermal conductivity
\dot{q}	Heat source term
Fo	Fourier number
Nu	Nusselt number
MW	Molecular weight
SC	Stoichiometric coefficient
β	Reaction plateau slope coefficient
α	Thermal diffusivity
E	Activation energy
ΔH	Reaction enthalpy
ΔS	Reaction entropy

1. INTRODUCTION

The intermittent nature of RES (mainly solar and wind power) poses multiple challenges as for their fully-fledged implementation, mainly related to the stability and the operations of the power systems [1-6]. Therefore, among other significantly important solutions, the large-scale implementation of an effective and efficient energy storage system is pivotal to overcome the above-mentioned issues [7-9].

In this wide and complex scenario, hydrogen has shown excellent potential as energy carrier [10] and as energy storage medium [11]. In fact, it can provide potentially carbon neutral, clean and secure energy to all sectors of the economy, including hard-to-abate ones (industry, transportation, and buildings) [12–16]. Such an extensive utilization of hydrogen (called as hydrogen economy) needs harmless, compact, light, and cost-efficient hydrogen storage [17]. The main hydrogen storage methods include gas, liquid, and solid storage [18] [19].

Among the latter methods, Metal Hydride (MH) hydrogen storage is one of the most promising solutions, especially for stationary applications [20]. Compared to physical-based storage, MHs are safer and more reliable, have higher hydrogen volumetric density, comparatively low operating pressure, and can operate at room temperature [21–24]. Nonetheless, none of the current MH technologies fulfills all the essential criteria for a practical hydrogen economy [17], especially due to their slow kinetics and the difficulty in controlling MH temperatures during hydrogen absorption and release. More specifically, being the hydrogen absorption (hydrogenation) and hydrogen desorption (dehydrogenation) to/from MH respectively exothermic and endothermic processes, the rate at which the hydrogen gas is absorbed can be maximized by lowering the system temperature, and the converse happens for the desorption process [25]. Therefore, advanced thermal control and management are crucial to enhance MH performance [26, 27]. Literature shows significant research and development efforts to improve heat transfer in the MH tanks, in order to efficiently operate alternate heating and cooling and obtain reaction times of practical interest. In particular, current research focuses on: (i) techniques to improve the effective thermal conductivity of the MH bed; (ii) design of high efficiency internal/external heat exchanger; (iii) Phase Change Materials (PCMs) utilization.

The latter is an elegant and efficient solution, in which the MH is thermally coupled with phase change materials that store and release heat in a narrow

temperature range through melting and solidification [28, 29], thus working as a thermal energy storage unit. Currently, various research investigates distinct aspects of MH-PCM coupling [30–32]. The purpose is to store all the heat released during the hydrogenation of the MH tank, thus minimizing the loading time and increasing the power performance of the reactor. To this end, the choice of an appropriate PCM and the optimization of its quantity are essential to ensure efficient heat transfer and fast hydrogen charge and discharge rates [33]. The PCM should have high thermal conductivity and melting enthalpy and a suited phase change temperature. In particular, the melting enthalpy should be equal or larger than the reaction enthalpy of MH [25], and the phase change temperature must be between the highest and lowest temperatures of the MH during charge/discharge processes [34]. In [35], the authors examine a MH-PCM system studying the PCM choice and evaluating the effect of several thermodynamic properties such as melting temperature, latent heat of fusion, specific heat capacity, density, and thermal conductivity. Especially, such last parameter is low for most PCMs [36] and an improvement is needed to enhance the heat exchange.

Most of the studies in this sector rely on 1D models, especially for cylindrical canisters with central arteries for the hydrogen delivery. Although this has notable practical advantages, it is important to highlight under what conditions the 2D phenomena cannot be neglected. This paper aims to find a guideline on how and when to neglect border effects or other phenomena which impair the 1D model accuracy. To the best of our knowledge, this problem has not been approached for a hybrid MH-PCM system, in which also the PCM domain is accurately modeled during its phase change.

The paper is organized as follows. In Section 2 we describe the system, the mathematical model, the domains discretization, and the heat exchange model. Results for the absorption and desorption processes are presented in Section 3 and discussed in Section 4. Finally, we draw the conclusions in Section 5.

2. METHODOLOGY

2.1 System description

The system is made of an inner MH cylinder of length \mathcal{L} and radius b_1 and porosity $\xi = 0.5$ surrounded by a hollow PCM cylinder of radius b_2 , as shown in Fig. 1. The selected MH is LaNi_5 , with a gravimetric density $\%wt$ of 1.40%. We assume that the system is thermally insulated (see [37]). Hydrogen flows to/from the MH canister through a 5mm diameter valve. We use a cylindrical

coordinate system (see Fig. 1) with the z axis along the canister length.

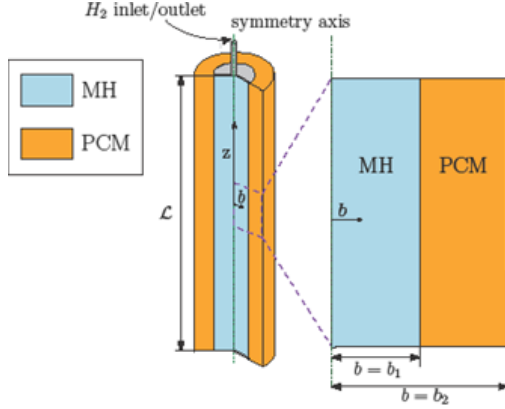


Fig. 1. The MH-PCM system configuration

A complete cycle consists of charge, dormancy, and a discharge phase (see Fig. 2).

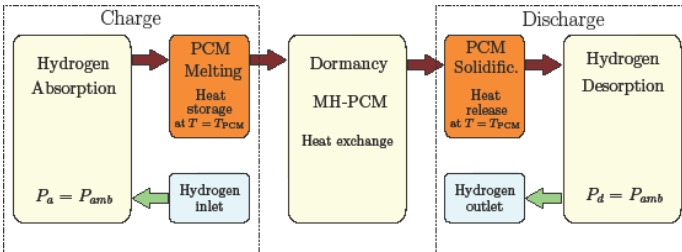


Fig. 2. The whole process in the MH-PCM storage system

The PCM serves as heat storage to passively control the MH temperature. Its melting/solidification temperature matches the MH equilibrium temperature at the selected storage pressure. Therefore, in charge, the hydrogenation heat flows from the MH to the PCM that melts at (almost) constant temperature. In this phase H_2 is provided to the system at a pressure p_{H_2} higher than the equilibrium pressure (p_{eq}).

Conversely during dehydrogenation, the PCM heats the MH using the thermal energy stored during hydrogenation. In this phase $p_{H_2} < p_{eq}$. In the dormancy phase, MH continues heating the PCM until a steady-state condition is reached (i.e., when the hydride has the same temperature of the PCM). The selected PCM is the salt $LiNO_3 - 3H_2O$.

2.2 Mathematical modeling

We construct a mathematically tractable system model under the following hypotheses: (i) all gases are ideal (see for instance [38]); (ii) the porous medium is homogeneous (see for instance [39]); (iii) both inlet/outlet hydrogen pressures are constant (see for instance [32]); (iv) the physical properties of MH/PCM are not functions of their temperature [40]; (v) the gas

pressure inside the vessel is uniform therefore no momentum conservation is accounted for [38]; (vi) the gas and the MH are locally in thermal equilibrium.

2.2.1 MH modeling

We discard all the irreversibilities which lower the system efficiency, such as the metal powder pulverization and self-densification [41] and we model the MH reversible dynamics through the mass and energy conservation equations as follows [42]:

$$\frac{dm_{H_2g}}{dt} = f_{H_2} - \frac{r m_{MH} M W_{H_2} S C}{M W_{MH}},$$

$$(\rho c_p)_e \frac{\partial T}{\partial t} = k_e \nabla^2 T + \dot{q},$$

being k_e the effective thermal conductivity, $(\rho c_p)_e$ the effective heat capacity, and \dot{q} the volumetric heat source. In turn, the effective conductivity k_e and heat capacity $(\rho c_p)_e$ are calculated as presented in [37, 43]. The hydride thermal conductivity, density, and specific heat are $k_{MH} = 2$ W/mK, $\rho_{MH} = 7260$ kg/m³, $c_{p_{MH}} = 419$ J/kgK. f_{H_2} is the hydrogen mass flow rate.

In absorption, the reaction rate r is:

$$r = C_a e^{-\frac{E_a}{RT}} \ln\left(\frac{p}{p_{eq}}\right) (1 - \phi),$$

while in desorption:

$$r = C_d e^{-\frac{E_d}{RT}} \frac{p - p_{eq}}{p_{eq}} \phi,$$

where ϕ is the saturation level ($0 < \phi < 1$). Finally, p_{eq} is calculated with the following equation:

$$p_{eq} = p_0 \exp\left[\frac{\Delta H}{RT} - \frac{\Delta S}{R} + \beta(\phi - 0.5)\right],$$

where $p_0 = 1$ bar is the reference pressure, ΔH and ΔS are the enthalpy, entropy variations respectively.

2.2.2 PCM modeling

During dehydrogenation, conduction is the leading heat exchange mechanism [43]. Therefore, we model the PCM solidification through the Enthalpy method (see for instance [44]). Conversely, during absorption and dormancy, the convection dominates the heat exchange within the PCM. Therefore, we model the PCM melting through a lumped parameter model where:

$$\dot{Q} = \frac{Nu k_{PCM}}{L} A (T_{surf} - T_{PCM}),$$

where \dot{Q} is the conduction heat, Nu is the Nusselt number, $A = 2\pi b_1 \mathcal{L}$ is the heat exchange surface, T_{surf} is the temperature at the MH/PCM interface, and $T_{PCM} = 305$ K is the PCM melting temperature. In turn, Nu can be expressed via the definition given in [26]. The volume of PCM V_{PCM} is selected on the basis of the reaction enthalpy, i.e.:

$$V_{PCM} = \frac{\%wt \cdot m_{MH} \cdot \frac{\Delta H}{MW_{H_2}}}{\lambda_{PCM}} \cdot \frac{1}{\rho_{PCM}},$$

where $\Delta H = 30$ kJ/mol is the reaction enthalpy, $\lambda_{PCM} = 300$ kJ/kg, and $\rho_{PCM} = 2100$ kg/m³.

2.3 Numerical solution

The energy conservation equation and the reaction rate equation (see [42]) are partial differential equations. To this aim, we express them according to the domains discretization. However, the discretization differs for the 1D and 2D models. The domain is axisymmetric in the 1D model; therefore, the nodes are placed between $b = 0$ (vessel core) and b_2 (external radius of the outer cylinder). In fact, the temperature varies in the radial direction and remains constant in the axial direction. The MH domain is discretized between $b = 0$ and b_1 (radius of the MH-PCM interface) while the PCM domain is discretized between b_1 and b_2 . For the PCM discretization.

Conversely, the nodes are placed both in the radial and axial direction in the 2D model. The MH and the PCM domain are also discretized along the z axis, adding the same number of z nodes in both domains, yielding a structured mesh. At the base of the canister a fixed temperature boundary condition is applied.

We use a second order finite difference scheme for the spatial discretization while the numerical solution of the differential and algebraic equations is implemented in Matlab R2020a.

3. MODEL VALIDATION

The model here presented is validated and compared with data in the literature. We simulate the absorption and desorption processes in a reactor with the same characteristics and operating conditions as those of the "small reactor" presented in the work of Laurencelle et al. [45]. The reactor contains 1 g of LaNi₅ and is charged at 6 bar and discharged at 0.068 bar. The reactor's external surface is kept at constant temperature through cooling and heating with water circulation loop. This enhances the reaction's kinetics. The parameters used for the simulation are those reported in [42], which followed the same validation

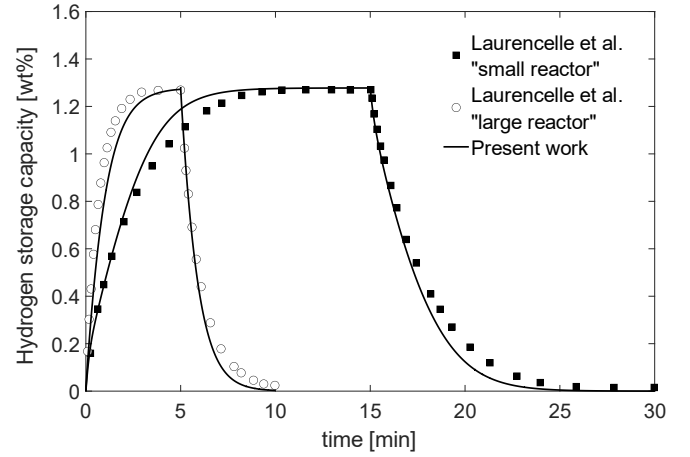


Fig.3 Validation of hydrogen storage capacity curves

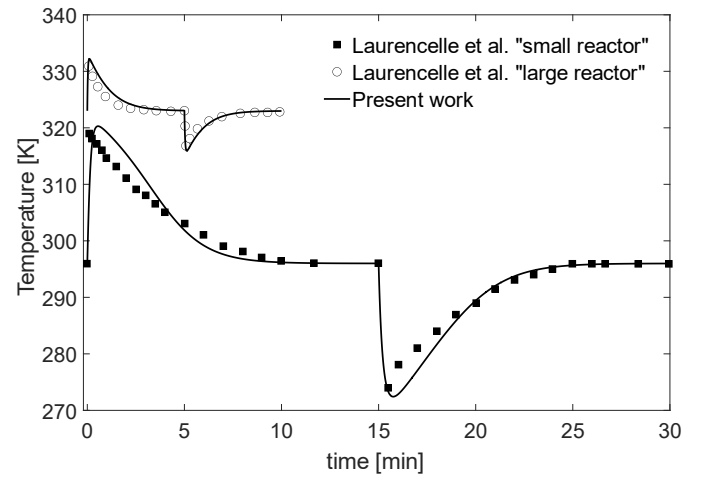


Fig. 4 Validation of reactor temperature curves

procedure. Table 1 presents the value of such parameters.

Table 1: simulation parameters used for validation [42,45]

Parameter	Value (abs/des)	
Thermal conductivity	2	W/mK
Density	8310	kg/m ³
Porosity	0.55	-
Specific heat	355	J/kgK
ΔH	-30,478 / 30,800	J/mol
ΔS	-108 / 108	J/molK
E	21,170 / 16,420	J/mol
C	59.2 / 9.6	1/s
SC	2.76	-

The time-dependent evolution of the hydrogen storage capacity and the corresponding average reactor

temperature are shown in Fig. 3 and Fig. 4, respectively. Both absorption and desorption processes are validated. Our numerical results are in good agreement with the averaged data reported by Laurencelle.

4. RESULTS AND DISCUSSION

The results are presented in non-dimensional terms to give generality to the analysis. The volume of the canister (and thus the amount of hydrogen stored) is kept equal throughout the different simulations. In particular, 1 kWh storage systems are compared, which corresponds to 30 g of stored H_2 .

4.1 Results

Fig. 5 and Fig. 6 show the non-dimensional absorption and desorption processes, respectively, where the 1D and 2D simulations are compared. The canister aspect ratio has a notable impact on the total time needed to absorb or desorb hydrogen and higher values correspond to quick reactions. This is due to the increased heat exchange surface between MH and PCM. In both phases, the total time needed for the process is not significantly different between 1D and 2D simulations, although in absorption the discrepancy is more relevant for low aspect ratios. However, especially in desorption and for low aspect ratios, the 1D and 2D curves significantly differ in the central part of the process. Then, the curves get progressively closer as they approach the final stages. This behaviour can be explained considering that the boundary condition imposed at the base of the canister fosters the reaction in the early stages. Fig.7 shows the non-dimensional temperature $T^* = T/T_{PCM}$ for different aspect ratios

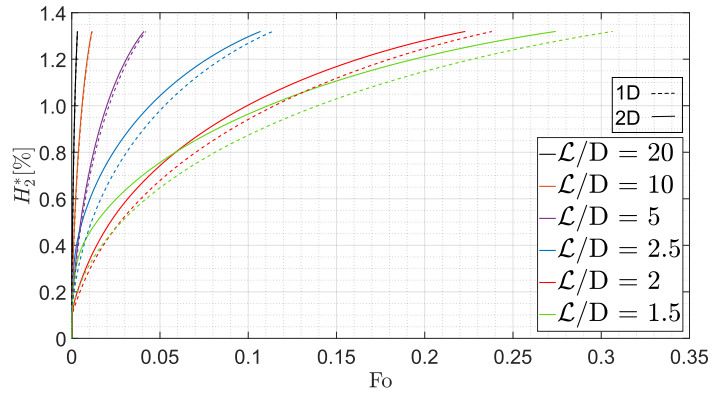


Fig. 5 Non-dimensional absorption for different aspect ratios

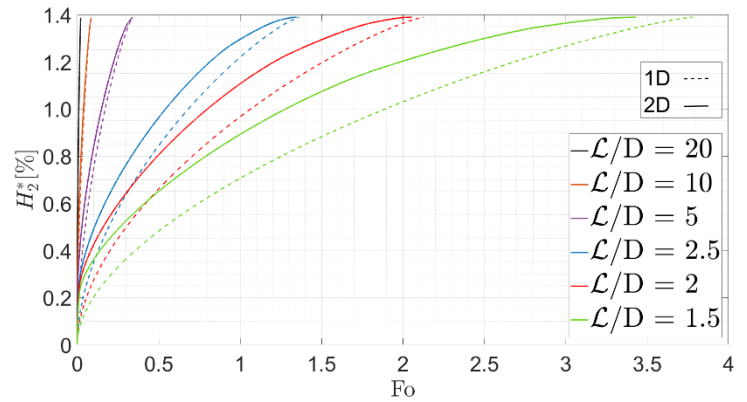


Fig. 6 Non-dimensional desorption for different aspect ratios at the end of the desorption process, where T_{PCM} is the melting temperature of the PCM. $\mathcal{R}^* = b/b_2$ is the non-dimensional radius. The higher the aspect ratio, the less relevant the influence of the z-axis derivative on the temperature distribution and, thus, on the reaction progress. It can also be noted that not all the PCM is in solid state at the end of desorption, thus suggesting that

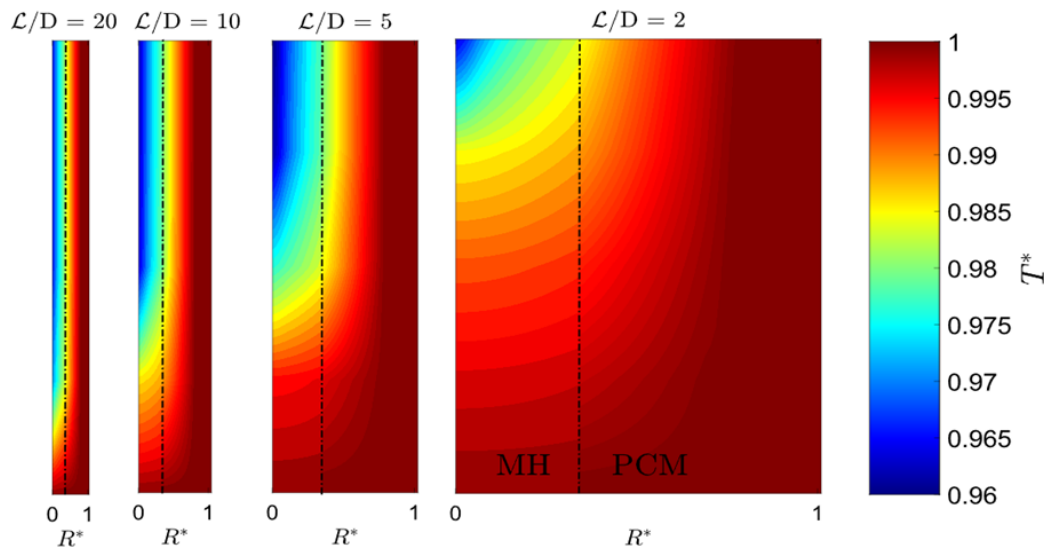


Fig. 7. Non-dimensional temperature distribution at the end of desorption for 4 different aspect ratios. The dash-dot line corresponds to the MH-PCM interface

the heat transfer is not fast enough to cause the complete solidification. In fact, the isothermal area at $T^* = 1$ corresponds to liquid cells. However, the heat exchange is progressively more intense for higher aspect ratios, which can be deduced by the relatively larger area at low temperature (i.e., $T^* < 0.98$). This was also deduced from Fig. 3 and Fig. 4.

In Fig. 8, the final Fo values for the desorption in the 1D and 2D simulations are compared. It is apparent how the reaction is not significantly influenced by the discretization method overall. Matter of fact, the discrepancy between 1D and 2D models is negligible in terms of global time needed for the hydrogen gas to desorb (Fo_{end}) when $L/D < 5$ and null for higher aspect ratios.

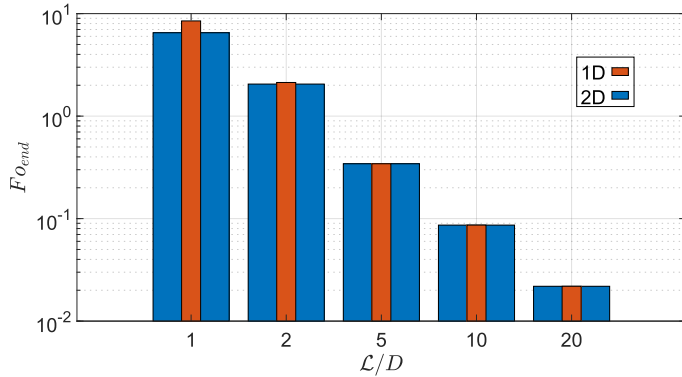


Fig. 8 Fo number at the end of desorption (Fo_{end}) for different aspect ratios

Fig. 9 shows how the non-dimensional equivalent output power $\mathcal{P}^* = \frac{\mathcal{P}D}{\alpha_{MH}^3 \rho_{MH} 10^{18}}$ distributes over the desorption process for different aspect ratios. $\mathcal{P} = f_{H_2} * H_i$ is the equivalent output power, where H_i is the hydrogen LHV; α_{MH} is the MH thermal diffusivity. Finally, $\phi = 1 - m_{H_2}/m_{tot}$ is the non-dimensional time (i.e., the state of charge/discharge), being m_{H_2} and m_{tot} the time-dependent and total stored hydrogen, respectively. The 10^{18} reduction factor is for ease of representation. The power curve has high values as long as less than 5% of hydrogen is desorbed. This phase corresponds to the choked flow rate, being the outlet pressure much lower than p_{H_2} . The transition to the almost-linear phase is smoother in the 2D model, as a result of the positive influence of the isothermal boundary condition imposed at the base of the canister. From Fig. 9 it is clear how higher aspect ratios correspond to higher output powers, due to the higher heat exchange rate between MH and PCM. Also, independently from the aspect ratio, the 2D model predicts a higher output power until about 40% of the

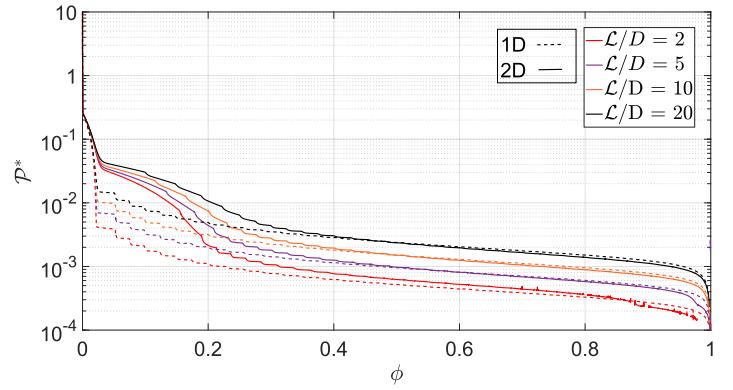


Fig. 9 Non-dimensional equivalent output power as function of ϕ for different aspect ratios

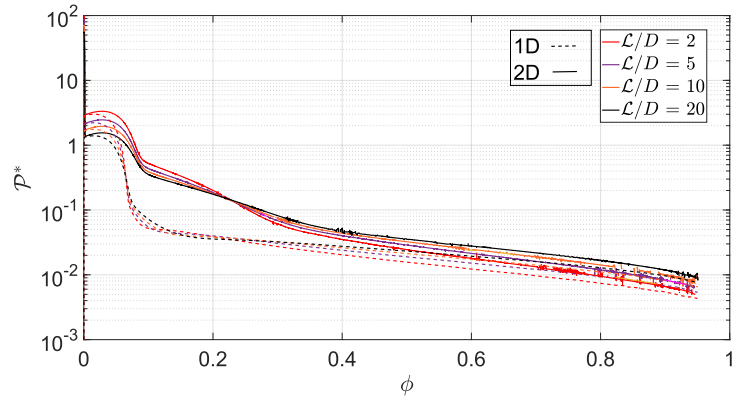


Fig. 10 Non-dimensional equivalent input power as function of ϕ for different aspect ratios

hydrogen has been released. Then, 1D and 2D models tend to converge. This is in accordance with the trends of Fig. 5 and 6, where the discrepancy in the first phase is barely visible due to the time scale of Fo with respect to ϕ .

In absorption, the discrepancy between 1D and 2D models in the first phase of the charge (i.e., up to 40% of absorbed hydrogen) is even more conspicuous (see Fig. 10). The input power is constantly higher than the output power, which is in accordance with the lower Fo number experimented in Fig. 5 compared to Fig. 6. In absorption the transition to the linear section of the curve is smoother in the 2D model as well as in desorption. Then, 1D and 2D curves tend to get closer. Note that for $\phi < 0.25$, the relation between L/D and \mathcal{P}^* is reversed in the 2D model, and lower aspect ratios have higher powers. This is due to diminished relevance of the fixed boundary condition for thin and long canisters. In the long run, this benefit vanishes and \mathcal{P}^* gets higher for higher aspect ratios. The critical ϕ is not a function of the aspect ratio.

4.2 Discussion

A critical value of 5 for the aspect ratio can be suitable when it comes to the discrimination between 1D and 2D numerical simulations of cylindrical MH-PCM systems. For lower values, thus shorter and thicker canisters, 2D numerical models are needed to thoroughly account for what happens within the temperature distribution, and thus the process evolution. For aspect ratios higher than 5, there is no practical difference between 1D and 2D simulations. However, if the total time of the processes is the only aspect of interest, note that no significant differences result from this analysis, since for both absorption and desorption processes, the global time of reaction is the same between 1D and 2D numerical models. Fig. 7 shows that finding novel solutions to deepen the conductive heat exchange inside the PCM is of utmost importance. Fins or metal foams are surely among the most promising solutions. Carbon nanoparticles may be diluted in the PCM as well, in order to increase the conductivity. Fig. 9 and Fig. 10 show that the absorption is notably faster than desorption, due to the convective nature of the heat exchange between MH and PCM, suggesting that putting effort into the development of a more sophisticated heat management during discharge has a higher impact on the overall efficiency of the system, rather than focusing on the charge process. Also, the fixed temperature boundary condition at the base of the canister proves to be of significant relevance when it comes to low aspect ratios, thus suggesting that securing thick canisters on a fixed temperature base can have notable benefits for this design.

5. CONCLUSIONS

Finding suitable, efficient, and safe energy storage systems is one of the key challenges of the energy transition. In this context, hydrogen storage systems will play an indisputable role, thanks to high energy density and flexibility with clean energy sources like solar and wind power. In this work we analyzed six cylindrical layouts of a hybrid Metal Hydride – Phase Change Material hydrogen storage system in terms of process time, temperature distributions, and output power. We found a critical value of 5 for the canister aspect ratio: for higher values, simple one-dimensional simulations can be conducted without impairing the results. Furthermore, the global time needed for the absorption and desorption reactions are not functions of the aspect ratio, except for extremely low values, e.g., $L/D < 2$. This suggests relying on one-dimensional models

especially when the time-dependent evolution of the processes is not needed.

The simulations may be repeated for different thermophysical properties of the materials (i.e., of MH and of PCM) to find evidence with respect to their influence on the critical value for the aspect ratio. Also, analyzing more complex and sophisticated geometries is of crucial importance to find novel solutions for reducing the total time of charge and discharge, e.g., finned design which increase the heat exchange between MH and PCM. Assessing the influence of the 2D phenomena on a longitudinal finned MH-PCM design may be one of the most urgent developments of this work.

ACKNOWLEDGEMENT

Progetto ECS 0000024 Rome Technopole, - CUP B83C22002820006, PNRR Missione 4 Componente 2 Investimento 1.5, finanziato dall'Unione europea – NextGenerationEU.

DECLARATION OF INTEREST STATEMENT

The authors declare that they have no known competing financial interests or personal relationships that could have appeared to influence the work reported in this paper. All authors read and approved the final manuscript.

REFERENCE

- [1] J. Li, J. Fang, Q. Zeng and Z. Chen, "Optimal operation of the integrated electrical and heating systems to accommodate the intermittent renewable sources," *Applied Energy*, vol. 167, p. 244–254, 2016.
- [2] M. A. Eltawil and Z. Zhao, "Grid-connected photovoltaic power systems: Technical and potential problems - A review," *Renewable and sustainable energy reviews*, vol. 14, p. 112–129, 2010.
- [3] M. Child, C. Kemfert, D. Bogdanov and C. Breyer, "Flexible electricity generation, grid exchange and storage for the transition to a 100% renewable energy system in Europe," *Renewable energy*, vol. 139, p. 80–101, 2019.
- [4] A. S. Anees, "Grid integration of renewable energy sources: Challenges, issues and possible solutions," in *2012 IEEE 5th India International Conference on Power Electronics (IICPE)*, 2012.
- [5] W. A. Omran, M. Kazerani and M. M. A. Salama, "Investigation of methods for reduction of power fluctuations generated from large grid-connected photovoltaic systems," *IEEE Transactions on Energy Conversion*, vol. 26, p. 318–327, 2010.

- [6] Y. Wu, T. Zhang, R. Gao and C. Wu, "Portfolio planning of renewable energy with energy storage technologies for different applications from electricity grid," *Applied Energy*, vol. 287, p. 116562, 2021.
- [7] D. Mohler and D. Sowder, "Energy Storage and the Need for Flexibility on the Grid," in *Renewable energy integration*, Elsevier, 2017, p. 309–316.
- [8] A. Rosati, A. L. Facci and S. Ubertini, "Techno-economic analysis of battery electricity storage towards self-sufficient buildings," *Energy Conversion and Management*, vol. 256, p. 115313, 2022.
- [9] J. Koskela, A. Rautiainen and P. Järventausta, "Using electrical energy storage in residential buildings—Sizing of battery and photovoltaic panels based on electricity cost optimization," *Applied energy*, vol. 239, p. 1175–1189, 2019.
- [10] M. A. Rosen and S. Koohi-Fayegh, "The prospects for hydrogen as an energy carrier: an overview of hydrogen energy and hydrogen energy systems," *Energy, Ecology and Environment*, vol. 1, p. 10–29, 2016.
- [11] F. Zhang, P. Zhao, M. Niu and J. Maddy, "The survey of key technologies in hydrogen energy storage," *International journal of hydrogen energy*, vol. 41, p. 14535–14552, 2016.
- [12] S. Ubertini, A. L. Facci and L. Andreassi, "Hybrid hydrogen and mechanical distributed energy storage," *Energies*, vol. 10, p. 2035, 2017.
- [13] A. L. Facci, D. Sánchez, E. Jannelli and S. Ubertini, "Trigenerative micro compressed air energy storage: Concept and thermodynamic assessment," *Applied Energy*, vol. 158, p. 243–254, 2015.
- [14] A. L. Facci, V. Cigolotti, E. Jannelli and S. Ubertini, "Technical and economic assessment of a SOFC-based energy system for combined cooling, heating and power," *Applied energy*, vol. 192, p. 563–574, 2017.
- [15] A. L. Facci and S. Ubertini, "Analysis of a fuel cell combined heat and power plant under realistic smart management scenarios," *Applied Energy*, vol. 216, p. 60–72, 2018.
- [16] G. Loreti, A. L. Facci, I. Baffo and S. Ubertini, "Combined heat, cooling, and power systems based on half effect absorption chillers and polymer electrolyte membrane fuel cells," *Applied Energy*, vol. 235, p. 747–760, 2019.
- [17] J. O. Abe, A. P. I. Popoola, E. Ajenifuja and O. M. Popoola, "Hydrogen energy, economy and storage: review and recommendation," *International journal of hydrogen energy*, vol. 44, p. 15072–15086, 2019.
- [18] L. Zhou, "Progress and problems in hydrogen storage methods," *Renewable and Sustainable Energy Reviews*, vol. 9, p. 395–408, 2005.
- [19] J. Xiao, R. Peng, D. Cossement, P. Bénard and R. Chahine, "CFD model for charge and discharge cycle of adsorptive hydrogen storage on activated carbon," *International journal of hydrogen energy*, vol. 38, p. 1450–1459, 2013.
- [20] S. D. Patil and M. R. Gopal, "Analysis of a metal hydride reactor for hydrogen storage," *International Journal of Hydrogen Energy*, vol. 38, p. 942–951, 2013.
- [21] S. Niaz, T. Manzoor and A. H. Pandith, "Hydrogen storage: Materials, methods and perspectives," *Renewable and Sustainable Energy Reviews*, vol. 50, p. 457–469, 2015.
- [22] L. Tong, Y. Yuan, T. Yang, P. Bénard, C. Yuan and J. Xiao, "Hydrogen release from a metal hydride tank with phase change material jacket and coiled-tube heat exchanger," *International Journal of Hydrogen Energy*, vol. 46, p. 32135–32148, 2021.
- [23] H. El Mghari, J. Huot and J. Xiao, "Analysis of hydrogen storage performance of metal hydride reactor with phase change materials," *International Journal of Hydrogen Energy*, vol. 44, p. 28893–28908, 2019.
- [24] B. Sakintuna, F. Lamari-Darkrim and M. Hirscher, "Metal hydride materials for solid hydrogen storage: a review," *International journal of hydrogen energy*, vol. 32, p. 1121–1140, 2007.
- [25] S. D. Lewis and P. Chippar, "Analysis of heat and mass transfer during charging and discharging in a metal hydride-phase change material reactor," *Journal of Energy Storage*, vol. 33, p. 102108, 2021.
- [26] A. L. Facci, M. Lauricella, S. Succi, V. Villani and G. Falcucci, "Optimized Modeling and Design of a PCM-Enhanced H₂ Storage," *Energies*, vol. 14, p. 1554, 2021.
- [27] S. Z. Baykara, "Hydrogen: A brief overview on its sources, production and environmental impact," *International Journal of Hydrogen Energy*, vol. 43, p. 10605–10614, 2018.
- [28] I. Dincer and M. A. Rosen, *Thermal energy storage systems and applications*, John Wiley & Sons, 2021.
- [29] H. Nazir, M. Batool, F. J. B. Osorio, M. Isaza-Ruiz, X. Xu, K. Vignarooban, P. Phelan, A. M. Kannan and others, "Recent developments in phase change materials for energy storage applications: A review," *International Journal of Heat and Mass Transfer*, vol. 129, p. 491–523, 2019.
- [30] S. Garrier, B. Delhomme, P. De Rango, P. Marty, D. Fruchart and S. Miraglia, "A new MgH₂ tank concept using a phase-change material to store the heat of reaction," *International journal of hydrogen energy*, vol. 38, p. 9766–9771, 2013.

[31] A. A. R. Darzi, H. H. Afrouzi, A. Moshfegh and M. Farhadi, "Absorption and desorption of hydrogen in long metal hydride tank equipped with phase change material jacket," *international journal of hydrogen energy*, vol. 41, p. 9595–9610, 2016.

[32] H. B. Maad, F. Askri and S. B. Nasrallah, "Heat and mass transfer in a metal hydrogen reactor equipped with a phase-change heat-exchanger," *International Journal of Thermal Sciences*, vol. 99, p. 271–278, 2016.

[33] H. El Mghari, J. Huot, L. Tong and J. Xiao, "Selection of phase change materials, metal foams and geometries for improving metal hydride performance," *International Journal of Hydrogen Energy*, vol. 45, p. 14922–14939, 2020.

[34] P. Marty, P. de Rango, B. Delhomme and S. Garrier, "Various tools for optimizing large scale magnesium hydride storage," *Journal of alloys and compounds*, vol. 580, p. S324–S328, 2013.

[35] S. Nyallang Nyamsi, I. Tolj and M. Lototskyy, "Metal hydride beds-phase change materials: Dual mode thermal energy storage for medium-high temperature industrial waste heat recovery," *Energies*, vol. 12, p. 3949, 2019.

[36] D. N. Nkwetta and F. Haghighat, "Thermal energy storage with phase change material-A state-of-the art review," *Sustainable cities and society*, vol. 10, p. 87–100, 2014.

[37] Y. Ye, J. Ding, W. Wang and J. Yan, "The storage performance of metal hydride hydrogen storage tanks with reaction heat recovery by phase change materials," *Applied Energy*, vol. 299, p. 117255, 2021.

[38] A. Chaise, P. de Rango, P. Marty and D. Frucharta, "Experimental and numerical study of a magnesium hydride tank," *International Journal of Hydrogen Energy*, vol. 35, pp. 6311-6322, 2010.

[39] Z. Bao, F. Yang, Z. Wu, X. Cao and Z. Zhang, "Simulation studies on heat and mass transfer in high-temperature magnesium hydride," *Applied Energy*, vol. 112, pp. 1181-1189.

[40] S. Mellouli, E. Abhilash, F. Askri and S. B. Nasrallah, "Integration of thermal energy storage unit in a metal hydride hydrogen storage tank," *Applied Thermal Engineering*, vol. 102, pp. 1185-1196, 2016.

[41] B. von Colbe et al., "Application of hydrides in hydrogen storage and compression: Achievements, outlook and perspectives," *international journal of hydrogen energy*, vol. 44, 2019.

[42] B. A. Talagañis, G. O. Meyer and P. A. Aguirre, "Modeling and simulation of absorption-desorption cyclic processes for hydrogen storage-compression using

metal hydrides," *International journal of hydrogen energy*, vol. 36, 2011.

[43] Y. Ye, J. Lu, J. Ding, W. Wang and J. Yan, "Numerical simulation on the storage performance of a phase change materials based metal hydride hydrogen storage tank," *Applied Energy*, vol. 278, p. 115682, 2020.

[44] V. VOLLER and M. Cross, "Accurate solutions of moving boundary problems using the enthalpy method," *International Journal of Heat and Mass Transfer*, vol. 24, 1981.

[45] F. Laurencelle and J. Goyette, "Simulation of heat transfer in a metal hydride reactor with aluminium foam," *International Journal of Hydrogen energy*, vol. 32, p. 2957 – 2964, 2007.